

Optimal Power Control for Real-Time Applications in Cognitive Satellite Terrestrial Networks

Shengchao Shi, Guangxia Li, Kang An, Zhiqiang Li, and Gan Zheng

Abstract—Cognitive satellite terrestrial networks have received considerable attention as a promising candidate to address the spectrum scarcity problem in future wireless communications. When satellite networks act as cognitive users in the networks, power control is a significant research challenge in the uplink case, especially for real-time applications. We propose two optimal power control schemes for maximizing the delay-limited capacity and outage capacity, respectively, which are useful performance indicators for real-time applications. From the long-term and short-term aspects, average and peak power constraints are adopted, respectively, at the satellite user to limit the harmful interference caused to the terrestrial base station. Extensive numerical results demonstrate the impact of interference constraints and channel condition parameters on the performance limits of satellite users.

Index Terms—Power control, satellite terrestrial networks, real-time applications, delay-limited capacity, outage capacity.

I. INTRODUCTION

SATELLITE networks play a significant role in future wireless communications due to their unique ability to provide seamless connectivity and high data rate. Compared with terrestrial cellular networks, satellite systems exhibit a prominent superiority for the inherent wide coverage and high reliability, especially in rural and sparsely populated areas [1], [2]. However, the continuous growth of broadband applications and multimedia services have resulted in an increasing demand for the spectrum in satellite communications. To address the spectrum scarcity, cognitive radio (CR) has recently received considerable attention in satellite communications, where two satellite networks or satellite terrestrial networks coexist within the same spectrum [3].

Among the existing applications of cognitive satellite systems, the case where the terrestrial system operates as primary network and the satellite system serves as secondary network has been proposed as a promising scenario from both academic and industry research [4]. In this regard, effective power control is a key enabling technique to alleviate the mutual interference and ensure the coexistence of two networks. Particularly, the authors of [5] investigate the power allocation schemes in downlink cognitive satellite terrestrial network,

Manuscript received December 29, 2016; revised February 19, 2017; accepted March 14, 2017. This work is supported by National Natural Science Foundation of China (No. 61571464, 61601511, 91338201, 91438109, and 61401507). The associate editor coordinating the review of this letter and approving it for publication was M. C. Aguayo-Torres. (*Corresponding author: Guangxia Li.*)

S. Shi, G. Li, K. An, and Z. Li are with the College of Communications Engineering, PLA University of Science and Technology, Nanjing 210007, China (e-mail: shishengchao88@gmail.com; satlab13905177686@163.com; ankang@nuaa.edu.cn; uuulzq@163.com).

G. Zheng is with the Wolfson School of Mechanical, Electrical, and Manufacturing Engineering, Loughborough University, Loughborough LE11 3TU, U.K. (e-mail: g.zheng@lboro.ac.uk).

Digital Object Identifier 10.1109/LCOMM.2017.2684798

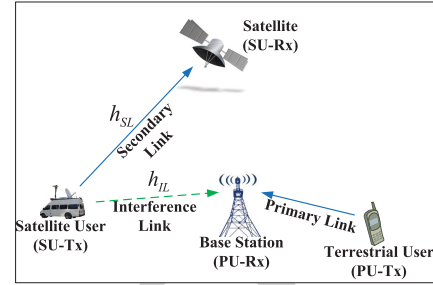


Fig. 1. Uplink cognitive satellite terrestrial network.

where the quality of service (QoS) provision of the terrestrial network is employed. Considering the uplink case, novel resource allocation schemes are proposed in [6], [7], where the terrestrial cellular system and fixed-service terrestrial microwave system serve as the primary networks, respectively. Nevertheless, these existing methods do not consider the real-time applications over practical propagation channels, which may require a constant rate transmission over all the fading blocks. Furthermore, the delay-sensitive service such as video transmission induces an emerging demand for future broadband Internet access. Therefore, it is an urgent research challenge to investigate the appropriate power control schemes for real-time applications in cognitive satellite terrestrial networks.

This letter presents two optimal power control schemes for the uplink cognitive satellite terrestrial networks. Since delay-limited capacity and outage capacity are key performance indicators for real-time applications [8], the proposed schemes aim to maximize the delay-limited capacity and outage capacity with different constraints while guaranteeing the communication quality of the primary terrestrial user. In addition, we provide closed-form solutions for the delay-limited capacity and the outage probability of the satellite user. Extensive numerical results evaluate the performance of the proposed schemes.

II. SYSTEM MODEL

The architecture of uplink cognitive satellite terrestrial network adopted in this letter is illustrated as shown in Fig. 1. In this network, the terrestrial cellular network acts as the primary system and shares the spectrum resource with the satellite network, which acts as the secondary system [6]. To improve the spectrum efficiency, we assume that the underlay technique is employed as the spectrum sharing approach, where the satellite user can share the same spectrum with the terrestrial user simultaneously without deteriorating its communication quality. Specifically, we assume that the terrestrial network is a Long-Term Evolution (LTE) system and the satellite network provides Digital Video Broadcasting - Satellite services to Handhelds (DVB-SH) system [5], [6].

As depicted in Fig. 1, h_{SL} and h_{IL} denote the channel power gains of the secondary satellite link and the terrestrial

interference link, respectively. Moreover, it is assumed that the interference from terrestrial terminal to the satellite can be considered to be negligible due to large distance [9]. For the secondary link, we employ the widely-adopted Shadowed-Rician fading model with closed formula, which can be used for mobile/fixed terminals operating in various propagation environment [5]. According to [10], the probability density function (PDF) of channel power gain h_{SL} is shown as

$$f_{h_{SL}}(h_{SL}) = \alpha \exp(-\beta h_{SL}) {}_1F_1(m_{SL}, 1, \delta h_{SL}), \quad (1)$$

where ${}_1F_1(\cdot, \cdot, \cdot)$ denotes the confluent hypergeometric function [11] and $\alpha = (2b_{SL}m_{SL}/(2b_{SL}m_{SL} + \Omega_{SL}))^{m_{SL}}/2b_{SL}$, $\beta = 1/2b_{SL}$, and $\delta = \Omega_{SL}/(2b_{SL}(2b_{SL}m_{SL} + \Omega_{SL}))$, with $2b_{SL}$ being the average power of the scatter component, Ω_{SL} the average power of the line-of-sight (LOS) component and m_{SL} the Nakagami fading parameter. For simplicity, we suppose that m_{SL} takes integer values. Under this situation, we adopt the identity [12, eq.(41)], and rewrite (1) as

$$f_{h_{SL}}(h_{SL}) = \frac{\alpha \sum_{k=0}^{m_{SL}-1} \frac{(-1)^k (1-m_{SL})_k (\delta h_{SL})^k}{(k!)^2}}{\exp((\beta - \delta)h_{SL})}. \quad (2)$$

As to the terrestrial interference link, Nakagami fading distribution is considered, which covers a wide range of fading scenarios for different values of the fading parameter. From [5], the channel power gain of h_{IL} follow the PDF given by

$$f_{h_{IL}}(h_{IL}) = \frac{\varepsilon^{m_{IL}} h_{IL}^{m_{IL}-1}}{\Gamma(m_{IL})} \exp(-\varepsilon h_{IL}), \quad (3)$$

where $\Gamma(\cdot)$ is the Gamma function [11], m_{IL} is the Nakagami fading parameter, Ω_{IL} is the average power and $\varepsilon = m_{IL}/\Omega_{IL}$. Furthermore, it is assumed that the perfect channel state information (CSI) about h_{SL} and h_{IL} is available for the satellite user. This can be accomplished by using training symbols for satellite link, and existing feedback link or spectrum manager (acts as a referee between the two systems) for terrestrial interference link¹ [6].

III. OPTIMAL POWER CONTROL SCHEMES

In this section, we propose two optimal power control schemes from the long-term and short-term perspectives, respectively. The long-term optimization aims to maximize the delay-limited capacity with average interference power constraints, while the short-term optimization maximizes the outage capacity with peak interference power constraints. In long-term power control scheme, the fading state is varying, whereas it is fixed in the short-term case.

A. Long-Term Optimal Power Control Scheme

For block fading channels, delay-limited capacity is defined as the maximum constant transmission rate over each of the fading blocks, which is a key performance metric for real-time applications [8]. To regulate the transmit power P_T of the satellite user in the long-term duration, average power constraints are commonly employed. Therefore, the long-term

¹The CSI may not be available to the satellite terminal due to the large distance, which requires necessary protection mechanism to eliminate the negative effects. Please note that this is still an open issue and beyond the topic of this letter, which will be our future work.

optimal power control scheme can be formulated as [8]

$$\begin{aligned} & \max_{P_T} B \log_2(1 + \gamma_s) \\ & s.t. \begin{cases} \gamma_s = \frac{P_T L_s G_t(\alpha) G_r(\varphi) h_{SL}}{N_{SL}} & (d1) \\ E(P_T L_p G_t(\alpha') G_{BS} h_{IL}) \leq I_{av} & (d2) \\ E(P_T) \leq P_{av} & (d3), \end{cases} \end{aligned} \quad (4)$$

where γ_s is the received signal-to-noise ratio (SNR) at the satellite, B and N_{SL} are the bandwidth and noise power, and $E(\cdot)$ denotes the statistical expectation. (d2) is the average interference power constraint adopted to guarantee a long-term QoS of primary user and (d3) is the average transmit power constraint. P_{av} and I_{av} denote the average transmit power limit and the average interference power limit, respectively. L_s and L_p are the free space loss of the secondary link and interference link. $G_t(\alpha)$ in (d1) corresponds to the transmit antenna gain at the satellite user for secondary link, which can be obtained as [7]

$$G_t(\alpha) = \begin{cases} G_{t,\max}, & 0^\circ < \alpha < 1^\circ \\ 32 - 25 \log \alpha, & 1^\circ < \alpha < 48^\circ \\ -10, & 48^\circ < \alpha < 180^\circ, \end{cases} \quad (5)$$

where α is the elevation angle. $G_t(\alpha')$ in (d2) denotes the equivalent transmit antenna gain for terrestrial interference link with off-axis angle $\alpha' = \arccos(\cos(\alpha) \cos(\beta))$ and β denotes the angle between the over horizon projected main lobe of the satellite user and the BS. Besides, G_{BS} is the receive antenna gain at the BS, and $G_r(\varphi)$ denotes the receive antenna gain at the satellite, which can be calculate as

$$G_r(\varphi) = G_{r,\max} \left(\frac{J_1(u)}{2u} + 36 \frac{J_3(u)}{u^3} \right)^2, \quad (6)$$

with $J(\cdot)$ being the Bessel function and $u = 2.07123 \frac{\sin \varphi}{\sin \varphi_{3dB}}$. $G_{r,\max}$ represents the maximum gain at the onboard antenna boresight, φ is the angle between the satellite user and the antenna boresight, and φ_{3dB} is the 3-dB angle [1] [12]. For simplicity, we denote $G_{SL} = L_s G_t(\alpha) G_r(\varphi)$ and $G_{IL} = L_p G_t(\alpha') G_{BS}$ in the rest of the derivation. Substituting (d1) into (d2) and (d3), we can get $\gamma_s \leq \frac{P_{av} G_{SL}}{N_{SL} E(\frac{1}{h_{SL}})}$ and $\gamma_s \leq$

$\frac{I_{av} G_{SL}}{N_{SL} G_{IL} E(\frac{h_{IL}}{h_{SL}})}$. According to the Jensen's inequality, it can

be directly concluded that $\frac{1}{E(h_{SL})} \leq E\left(\frac{1}{h_{SL}}\right)$. Therefore, γ_s satisfies $\gamma_s \leq \frac{P_{av} G_{SL}}{N_{SL}} E(h_{SL})$ and $\gamma_s \leq \frac{I_{av} G_{SL}}{N_{SL} G_{IL} E(h_{IL})} E(h_{SL})$, i.e. $\gamma_s \max = \min \left\{ \frac{P_{av} G_{SL}}{N_{SL}} E(h_{SL}), \frac{I_{av} G_{SL}}{N_{SL} G_{IL} E(h_{IL})} E(h_{SL}) \right\}$. The delay-limited capacity C_{dl} can thus be calculated approximately as below

$$C_{dl} \approx \min \left\{ B \log_2 \left(1 + \frac{P_{av} G_{SL} E(h_{SL})}{N_{SL}} \right), B \log_2 \left(1 + \frac{I_{av} G_{SL} E(h_{SL})}{N_{SL} G_{IL} E(h_{IL})} \right) \right\}, \quad (7)$$

where by applying [11, eq.(3.351.3)] and (3), $E(h_{SL})$ and $E(h_{IL})$ can be respectively obtained as

$$E(h_{SL}) = \alpha \sum_{k=0}^{m_{SL}-1} \frac{(-1)^k (1-m_{SL})_k \delta^k (k+1)!}{(k!)^2 (\beta - \delta)^{k+2}}, \quad (8a)$$

$$E(h_{IL}) = \frac{m_{IL}}{\varepsilon} = \Omega_{IL}. \quad (8b)$$

B. Short-Term Optimal Power Control Scheme

Outage capacity is defined as the maximum rate that can be maintained over the fading blocks with a given outage probability [8]. That is to say, the minimum outage probability is closely related to the capacity. From a mathematical viewpoint, calculating outage capacity is equivalent to minimize the outage probability for a given outage capacity R_{th} . To manage P_T at each fading state, peak power constraints are more suitable in the short-term duration. Thus, the problem of short-term power control can be formulated as

$$\begin{aligned} \min_{P_T} Pr \left\{ B \log_2 \left(1 + \frac{P_T G_{SL} h_{SL}}{N_{SL}} \right) < R_{th} \right\} \\ \text{s.t.} \begin{cases} P_T G_{IL} h_{IL} \leq I_{\max} & \text{(t1)} \\ P_T \leq P_{\max} & \text{(t2)}, \end{cases} \end{aligned} \quad (9)$$

where $Pr \{ \cdot \}$ denotes the probability. (t1) and (t2) are peak interference power constraint and peak transmit power constraint, respectively. P_{\max} and I_{\max} are the corresponding peak transmit power limit and peak interference power limit. By solving (9), we can get the optimal transmit power as (10). Substituting (10) into (9), we can further obtain the outage probability as (11), where by using [11, eq.(3.351.1)], I_1 can be first expressed as

$$I_1 = \frac{1}{\Gamma(m_{IL})} \gamma \left(m_{IL}, \frac{\varepsilon I_{\max} G_{SL} h_{SL}}{G_{IL} N_{SL} (2^{R_{th}/B} - 1)} \right), \quad (12)$$

where $\gamma(\cdot, \cdot)$ is lower incomplete Gamma function [11]. Then, by substituting (12) into (11) and applying [11, eq.(8.352.1)], (11) can be rewritten as (13), as shown at the bottom of the page. To solve (13), we employ [11, eq.(3.351.2)] and calculate the integrals I_2 and I_3 as

$$I_2 = \frac{\Gamma \left(k + 1, (\beta - \delta) \frac{N_{SL} (2^{R_{th}/B} - 1)}{G_{SL} P_{\max}} \right)}{(\beta - \delta)^{k+1}}, \quad (14)$$

$$P_T = \begin{cases} \frac{N_{SL} (2^{R_{th}/B} - 1)}{G_{SL} h_{SL}}, & h_{SL} \geq \frac{N_{SL} (2^{R_{th}/B} - 1)}{G_{SL} P_{\max}} \text{ and } h_{IL} \leq \frac{G_{SL} h_{SL} I_{\max}}{G_{IL} N_{SL} (2^{R_{th}/B} - 1)}; \\ 0, & \text{others.} \end{cases} \quad (10)$$

$$P_{out} = 1 - \int_{\frac{N_{SL} (2^{R_{th}/B} - 1)}{G_{SL} P_{\max}}}^{\infty} \underbrace{\int_0^{\frac{G_{SL} h_{SL} I_{\max}}{G_{IL} N_{SL} (2^{R_{th}/B} - 1)}} f_{h_{IL}}(h_{IL}) dh_{IL} f_{h_{SL}}(h_{SL}) dh_{SL}}_{I_1}. \quad (11)$$

$$\begin{aligned} P_{out} = 1 - \alpha \sum_{k=0}^{m_{SL}-1} \frac{(-1)^k (1 - m_{SL})_k \delta^k}{(k!)^2} & \left\{ \underbrace{\int_{\frac{N_{SL} (2^{R_{th}/B} - 1)}{G_{SL} P_{\max}}}^{\infty} h_{SL}^k \exp(-(\beta - \delta) h_{SL}) dh_{SL}}_{I_2} \right. \\ & \left. - \sum_{m=0}^{m_{IL}-1} \frac{1}{m!} \left(\frac{\varepsilon G_{SL} I_{\max}}{G_{IL} N_{SL} (2^{R_{th}/B} - 1)} \right)^m \underbrace{\int_{\frac{N_{SL} (2^{R_{th}/B} - 1)}{G_{SL} P_{\max}}}^{\infty} h_{SL}^{m+k} \exp \left(- \left(\beta - \delta + \frac{\varepsilon G_{SL} I_{\max}}{G_{IL} N_{SL} (2^{R_{th}/B} - 1)} \right) h_{SL} \right) dh_{SL}}_{I_3} \right\}. \end{aligned} \quad (13)$$

$$I_3 = \frac{\Gamma \left(m+k+1, \left(\beta - \delta + \frac{\varepsilon G_{SL} I_{\max}}{G_{IL} N_{SL} (2^{R_{th}/B} - 1)} \right) \frac{N_{SL} (2^{R_{th}/B} - 1)}{G_{SL} P_{\max}} \right)}{\left(\beta - \delta + \frac{\varepsilon G_{SL} I_{\max}}{G_{IL} N_{SL} (2^{R_{th}/B} - 1)} \right)^{m+k+1}}, \quad (15)$$

where $\Gamma(\cdot, \cdot)$ is upper incomplete Gamma function [11].

IV. NUMERICAL RESULTS

To evaluate the performance of the proposed schemes, numerical results are presented in this section. In the simulations, we consider $B = 10\text{MHz}$, $\alpha = 10^\circ$, $\beta = 50^\circ$, $G_{r,\max} = 52.1\text{dB}$, $G_{t,\max} = 42.1\text{dB}$, $G_{BS} = 0\text{dB}$, satellite link distance $d_s = 36000\text{Km}$, interference link distance $d_p = 10\text{Km}$, noise temperature $T = 300\text{K}$ and $R_{th} = 35\text{Mbps}$ are assumed unless otherwise stated [1], [7]. Besides, three shadowing scenarios of the satellite link are considered, namely, Infrequent Light Shadowing (ILS), Frequent Heavy Shadowing (FHS) and Average Shadowing (AS). The typical values of satellite channel parameters can be obtained from Table III of [10]. It is notable that m_{IL} and m_{SL} take integer values when calculating the outage probability.

A. Delay-Limited Capacity

Fig. 2 shows the delay-limited capacity of the satellite user versus I_{av} for different P_{av} constraints, where the average shadowing is considered for the satellite link and the terrestrial channel parameters are $m_{IL} = 3$ and $\Omega_{IL} = 1.5$. It can be seen that the delay-limited capacity increases with I_{av} . However, the delay-limited capacity will get saturated when I_{av} is large enough. This is because the satellite user would transmit with its maximum available power P_{av} in this case. Therefore, the saturated value of the delay-limited capacity significantly increases with P_{av} .

Fig. 3 depicts the delay-limited capacity of the satellite user versus I_{av} for different shadowing scenarios of the satellite link. The results indicate that the delay-limited capacity

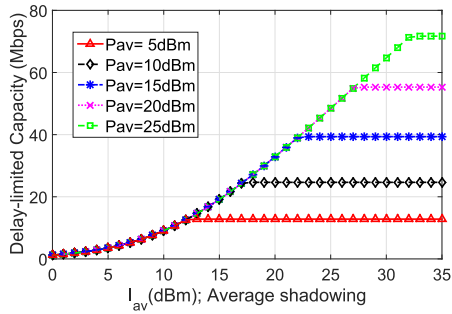


Fig. 2. Delay-limited capacity versus I_{av} for different P_{av} .

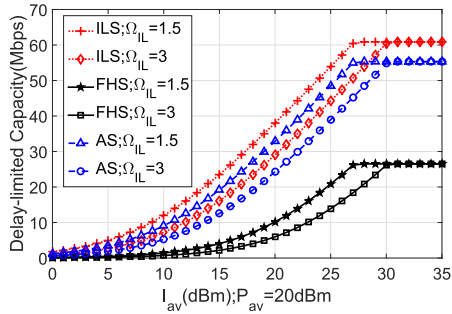


Fig. 3. Delay-limited capacity versus I_{av} for different shadowing scenarios of satellite link.

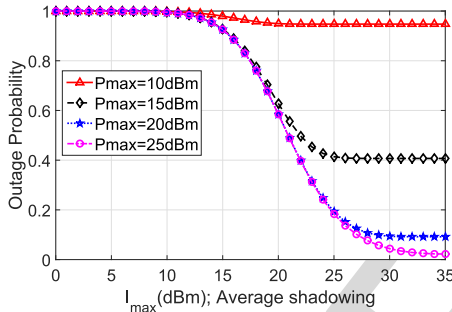


Fig. 4. Outage probability versus I_{max} for different P_{max} .

would increase when the satellite link experiences the weaker shadowing conditions. In addition, given the specific satellite link condition, the delay-limited capacity decreases with the increasing of Ω_{IL} . This is due to the fact that the interference link channel becomes stronger with Ω_{IL} increasing. That is to say, under the same I_{av} , the satellite user can transmit less power with the increase of Ω_{IL} .

B. Outage Capacity

The outage probability of satellite user versus I_{max} for different P_{max} constraints is illustrated in Fig. 4. From this figure, we can see that the outage probability decreases with the increasing of I_{max} and becomes saturated once I_{max} is large enough. Moreover, the saturated value of outage probability decreases when P_{max} increases. These conclusions are consistent with the findings in Fig. 2.

Fig. 5 shows the outage probability of satellite user versus I_{max} for different shadowing scenarios with $P_{max} = 20$ dBm. Similarly, the outage probability decreases when the satellite link channel condition improves. Since larger values of m_{IL} correspond to less severe fading conditions of the interference link, the outage probability decreases with the increase of m_{IL} for the same satellite link condition. However, the saturated values are identical due to the same peak power limit P_{max} .

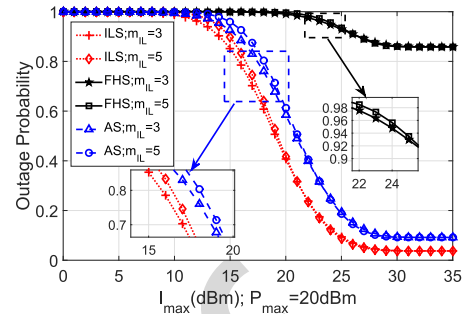


Fig. 5. Outage probability versus I_{max} for different shadowing scenarios of satellite link.

V. CONCLUSIONS

In this letter, we propose two optimal power control schemes for real-time applications in cognitive satellite terrestrial networks, which aim at maximizing the delay-limited capacity and outage capacity without degrading the communication quality of the primary terrestrial user. Average power and peak power constraints are employed from long-term and short-term perspectives, respectively. The impact of transmit power limits, interference power constraints, satellite link shadowing conditions and terrestrial interference link fading severity on the performance limits of the satellite user are demonstrated by extensive numerical simulations. In future works, we will investigate the impact of propagation delay on the performance of cognitive satellite terrestrial networks.

REFERENCES

- [1] G. Zheng, *et al.* "Generic optimization of linear precoding in multibeam satellite systems," *IEEE Trans. Wireless Commun.*, vol. 11, no. 6, pp. 2308–2320, Jun. 2012.
- [2] K. An *et al.*, "Performance analysis of multi-antenna hybrid satellite-terrestrial relay networks in the presence of interference," *IEEE Trans. Commun.*, vol. 63, no. 11, pp. 4390–4404, Nov. 2015.
- [3] S. K. Sharma *et al.* "Cognitive radio techniques for satellite communication systems," in *Proc. IEEE 78th VTC Fall*, Las Vegas, NV, USA, Sep. 2013, pp. 1–5.
- [4] K. Liolis *et al.*, "Cognitive radio scenarios for satellite communications: The CoRaSat approach," in *Proc. Future Netw. Mobile Summit*, Lisbon, Portugal, Jul. 2013, pp. 1–10.
- [5] S. Vassaki *et al.* "Power allocation in cognitive satellite terrestrial networks with QoS constraints," *IEEE Commun. Lett.*, vol. 17, no. 7, pp. 1344–1347, Jul. 2013.
- [6] S. Vassaki *et al.* "Optimal iSINR-based power control for cognitive satellite terrestrial networks," *Trans. Emerg. Telecommun. Technol.*, vol. 28, no. 2, pp. 1–10, Feb. 2017, doi: 10.1002/ett.2945.
- [7] E. Lagunas *et al.* "Power and rate allocation in cognitive satellite uplink networks," in *Proc. IEEE ICC*, Kuala Lumpur, Malaysia, May 2016, pp. 1–6.
- [8] X. Kang *et al.* networks: Ergodic capacity and outage capacity," *IEEE Trans. Wireless Commun.*, vol. 8, no. 2, pp. 940–950, Feb. 2009.
- [9] S. K. Sharma *et al.* "Satellite cognitive communications: Interference modeling and techniques selection," in *Proc. 6th ASMS, 12th SPSC*, Baiona, Spain, Sep. 2012, pp. 111–118.
- [10] A. Abdi *et al.* "A new simple model for land mobile satellite channels: First- and second-order statistics," *IEEE Trans. Wireless Commun.*, vol. 2, no. 3, pp. 519–528, May 2003.
- [11] I. S. Gradshteyn and I. M. Ryzhik, *Table of Integrals, Series, and Products*, 7th ed. Amsterdam, The Netherlands: Elsevier, 2007.
- [12] K. An *et al.* "Secure transmission in cognitive satellite terrestrial networks," *IEEE J. Sel. Areas Commun.*, vol. 34, no. 11, pp. 3025–3037, Nov. 2016.
- [13] K. An *et al.* "On the performance of multiuser hybrid satellite-terrestrial relay networks with opportunistic scheduling," *IEEE Commun. Lett.*, vol. 19, no. 10, pp. 1722–1725, Oct. 2015.